World Academy of Science, Engineering and Technology
International Journal of Mechanical and Mechatronics Engineering
Vol:7, No:1, 2013

A Strategy for a Robust Design of Cracked Stiffened Panels

Francesco Caputo, Giuseppe Lamanna, and Alessandro Soprano

***Abstract*—**This work is focused on the numerical prediction of the fracture resistance of a flat stiffened panel made of the aluminium alloy 2024 T3 under a monotonic traction condition. The performed numerical simulations have been based on the micromechanical Gurson-Tvergaard (GT) model for ductile damage. The applicability of the GT model to this kind of structural problems has been studied and assessed by comparing numerical results, obtained by using the WARP 3D finite element code, with experimental data available in literature. In the sequel a home-made procedure is presented, which aims to increase the residual strength of a cracked stiffened aluminum panel and which is based on the stochastic design improvement (SDI) technique; a whole application example is then given to illustrate the said technique.

***Keywords*—**Residual strength, R-Curve, Gurson model, SDI.

I. Introduction

THE definition of prediction tools of the residual strength curve (R-curve) of cracked structures is a very interesting task to improve the chance to investigate on some basic fracture resistance aspects of the material behaviour. The approach considered within this work is a micromechanical one, based on continuum mechanics by considering the numerical model as independent from the geometry of a generic cracked component, which is able to describe the material behaviour from the initial damage conditions up to the final collapse. Ductile fracture begins in many metal alloys with the nucleation of cavities induced by the brittle breaking or decohesion of inclusions [1], [2]. As these cavities grow in size, they generate local intense stress-strain fields around near small inclusions, thereby nucleating small-scale cavities which participate to the final phase of the coalescence process and therefore to the macroscopic crack growth. The process of cavity growth is well understood and the relative models are quite advanced [3], [4], while the mechanism of nucleation and coalescence, as well as the associated micromechanics, are less well understood even if some papers provide a good description of such mechanisms [5], [6]. It is clear that improving the understanding of the above mechanisms and of their effects on failure modes and fracture resistance will result in a better ease to develop micromechanical prediction tools for the analysis of real components which behave in the nonlinear fracture mechanics field. In this work we have selected the micromechanical model introduced by Gurson [7] in the version modified by Tvergaard [8], whose parameters have been determined by using both experimental data from metallurgical observations provided from literature [9] and a phenomenological home-made fitting procedure which required combined experimental [10] and numerical simulations.

The generally adopted structural optimization methods [11], [12] aim to minimize one or more functions in presence of prescribed boundary conditions and with reference to the possible ranges where the some of the design variables are defined; at the same time the other structural parameters are considered as constant. Such a design process cannot take into account the scattering of those parameters which randomly influence both the manufacturing process and the service conditions and which, in turn, induce heavy effects on the variability of the performance of the design product [13]. That consideration clarifies the requirement of a special design methodology, based on probabilistic concepts, as well as complete with procedures and practical tools such as to make possible to explore in detail the probabilistic aspects involved in the design process of an industrial product [14] in such a way as to obtain a robust design whose behaviour is rather insensitive to all variations of the main variables, or, what is the same, a design whose statistics are characterized by the smallest standard deviation, as a function of the statistics of input [15].

In most recent years, in the field of the structural design the definition of robust design has been subject to a reanalysis, which has resulted in a new design technique called “stochastic design improvement” (SDI) [16]. The initial objective of the reduction of the standard deviation of the output has been replaced by the fulfilment of an assigned condition (target), defined by engineering or marketing considerations, to be reached within an assigned probability value.

In this work a home-made procedure has been developed, based on the SDI technique, which is able to perform a preliminary robust design of a complex structural component; this procedure is illustrated with reference to the case of a stiffened aeronautical panel [10], whose residual strength in presence of cracks has to be improved [17]. Numerical results on the reference component have been validated by using experimental results from literature [18].

II. Description of the Home Made SDI Procedure

Perhaps the most used method to perform a probabilistic analysis of the behaviour of a complex structural component is Monte-Carlo (M-C) procedure, if necessary modified by using one among the variance reduction techniques in order to keep the number of necessary trials within an acceptable number.

On the other hand, in the case of optimization a M-C procedure based on a first trial assumption for the design variables gives a “cloud” of results, which is centred around a value which usually doesn’t coincide with the target; the SDI technique is based on the assumption that the same cloud can be displaced toward the desired position, i.e. in

The Authors are with the Department of Industrial and Information Engineering, the Second University of Naples, 81031 Aversa, Italy (e-mail: giuseppe.lamanna@unina2.it).

such a way as to be centred around the target, by varying only the mean value of the design variables and that the amplitude of the required displacement can be forecast through a close analysis of the points which are in the cloud, assuming that the shape and size of the cloud don't change greatly if the displacement is small enough: it is therefore immediate to realize that an SDI process is composed by several sets of MC trials (runs) with intermediate estimates of the required displacement. It is also clear that the assumption about the invariance of the cloud can be maintained just in order to carry out the multivariate regression which is needed to perform a new step but that subsequently a new and more correct evaluation of the cloud is needed. The displacement of the cloud is obtained by changing the statistics of the design variables and in particular by changing their mean (nominal) values, as in the now available version of the method all distributions are assumed to be uniform, to avoid the gathering of results around the mode value. It is also pointed out that sometimes the process could fail to perform its task because of some physical (engineering) limit, but in any case SDI allows to quickly appreciate the feasibility of a specific design, therefore making its improvement easier.

It may also happen that other stochastic variables are present in the problem (the so called background variables): they can be characterized by any type of statistical distribution, but they are not modified during the process. From a practical standpoint, the designer specifies the value that an assigned output variable has to reach and the SDI process determines those values of the project variables which ensure that the objective variable becomes equal, in the mean sense, to the target. Therefore, the user defines, according to the requirements of the problem, a set of variables as control variables, which are then characterized from an uniform statistical distribution (natural variability) within which the procedure can let them vary, observing the corresponding physical (engineering) limits. In the case of a single output variable, the procedure evaluates the Euclidean or Mahalanobis distance of the objective variable from the target after each trial. Then, it is possible to find among the worked trials that one for which the said distance gets the smallest value: subsequently the procedure redefines each project variable according to a new uniform distribution with a mean value equal to that used in such "best" trial. The limits of natural variability are accordingly moved of the same quantity of the mean in such way as to save the amplitude of the physical variability. Once the project variables have been redefined a new run is performed and the process restarts up to the completion of the assigned number of shots. It is possible to plan a criterion of arrest in such way as to make the analysis stop when the distance from the target reaches a given value. In the most cases, it is desirable to control the state of the analysis with a real-time monitoring with the purpose to realize if a satisfactory condition has been obtained.

III. Test Case

The procedure described above has been applied on a flat cracked and stiffened panel (Fig. 1).

The full panel is constituted by a skin made of Al alloy 2024 T3 LT, divided in three bays by four stiffeners made of Al alloy 7075 T5 L (see Table I). The longitudinal size (along the applied displacement) of the panel is 1830 mm, the transversal size is 1190 mm and the nominal thickness is 1.27 mm; the stiffeners are 2.04 mm high and 45 mm width. The stiffeners were connected to the skin by 4.0 mm diameter rivets (protruding head type), and a continuous rivet pattern was used [19]-[21]. Each stiffener was connected to the skin by two rows of rivets in the longitudinal direction. The distance between the stringers is 340 mm (Fig. 1). In general many aspects are involved in the mechanical joints as refer the authors in [22], [23]; in this application it was not taken into account all such features but only a part of them through preliminary numerical analyses. As result of such analyses, in the following it has been chosen to consider the skin and the stringers joined as a single component.

TABLE I
Material Properties

Material	E [MPa]	σ_y [MPa]	σ_u [MPa]	Δ_{ult} [%]
2024 T3 LT	71100	366	482	18
7075 T5 L	67000	525	579	16

Two different cracked panels have been considered with a central lead through crack equal to 120 and 150 mm respectively. The full panels were tested by [18] by using a vertical hydraulic actuator with a maximum load capacity of 1000 kN. A double-bridge load cell was mounted at the rod of the actuator. The applied loads were controlled by a typical closed-loop servo system. The stiffened panel was clamped to the testing machine frames by 29 pins per side (20 mm diameter, Fig. 2); the stress field around pins does not reach the bearing strength of the stiffener material. Fig. 2 shows a scheme of panel mounted in the testing frame. Tensile rods were used to prevent horizontal deflection of the frame during loading with care given to the assembly process [24]. The residual strength tests were done under displacement control to make the crack statically grow beyond the point of maximum load. During the residual strength test, the displacement was gradually increased until failure of the panel.

After the experimental tests were completed, a finite element model has been developed and analysed by using the WARP 3D FE code. The numerical model consists of no. 8400 8-noded 3-dof solid elements and 11450 nodes, only an eighth of the whole structure has been analysed due to the three symmetry planes. Classical metal plasticity models have been adopted: Mises yield surfaces with associated plastic flow, which allow for isotropic yield. Isotropic hardening behaviour has been considered according the mechanical characteristics reported in Table I.

Boundary conditions and crack dimensions were the same of experimental test.

The surrounding zone of the crack has been modelled by means of the Gurson-Tvergaard isotropic constitutive model for progressively cavitating elastic-plastic solids. The progressive degradation of the material strength properties in the fracture process zone due to micro-void growth to coalescence is modelled through the computational cell

concept suitable for quasi-static ductile fracture processes. Such constitutive model needs a calibration phase reported in the following paragraph.

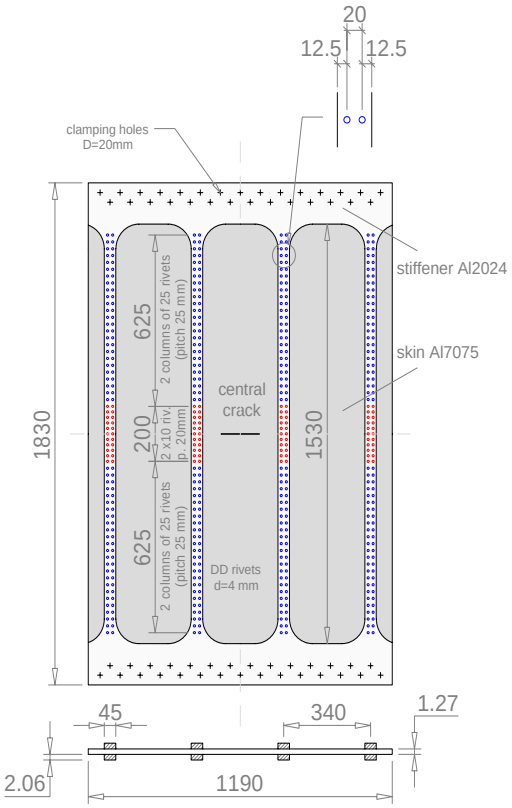

Fig. 1 Flat stiffened panel

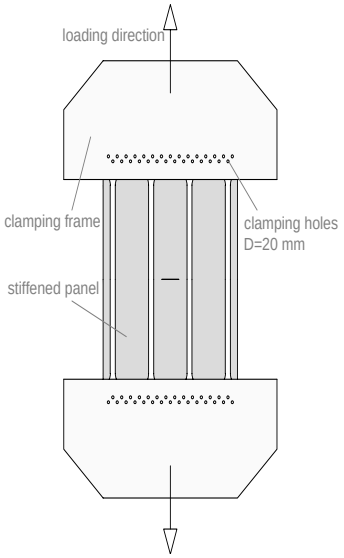

Fig. 2 Testing machine scheme

IV. Numerical Calibration of the GT Model Parameters

As it is well known, the Gurson-Tvergaard (GT) model [7], [8] is represented by the following expression (1)

$$\phi(q,\sigma_0,f,\sigma_m)= \frac{\sigma^2}{\sigma_0^2}+2q_1 f\cosh\left(\frac{3q_2\sigma_m}{2\sigma_0}\right)-1-q_3 f^2=0 \quad (1)$$

where f is the actual void volume fraction ($f = f_0$ at $t = 0$), σ_m is the hydrostatic pressure, σ is the equivalent Von Mises stress, σ_0 is the yielding stress of the material, q_1, q_2 and q_3 are the Tvergaard correction factors. The void volume fraction rate, df, consists of two terms, $df_{nucleation}$ and df_{growth}, respectively linked to the nucleation and the growth of voids. Void coalescence is assumed to start beyond a certain value of f, say f_c, and a macroscopic crack appears when the material ligaments between voids loose completely their capacity to carry a load whatever. From a numerical point of view, "computational cells", which implement the GT model, are positioned adjacent to the crack propagation plane and are numerically characterized by means of the aforesaid parameters. The numerical characterization of the computational cell, obviously, determines the size of the finite elements used to model the area around the crack tip, by considering one finite element for each cell. Nine parameters need to be calibrated (by means of a fitting procedure of numerical results with experimental ones) in order to fully characterize the computational cell in the sense above: the three Tvergaard correction parameters (q_1, q_2 q_3); the three parameters associated with the strain normal distribution (mean value, ε_n, standard deviation, S_N, and the volume fraction of void nucleating particles, f_N), which are assumed to govern the strain induced voids nucleation rate on the basis of the following expressions (2):

$$df_{nucleation} = A\left(\bar{\varepsilon}\right)d\bar{\varepsilon}_p$$
$$A=\frac{f_N}{S_N\sqrt{2\pi}}\exp\left[-\frac{1}{2}\left(\frac{\bar{\varepsilon}_p-\varepsilon_N}{S_N}\right)^2\right] \quad (2)$$

where $\bar{\varepsilon}_p$ is the equivalent plastic strain, D_0 is the initial size of the computational cell and f_0 is the initial volume cavity fraction which can reach its critical value f_c. Another purely numerical parameter, λ, has been considered, which governs the release model for element forces after the void volume fraction reaches the critical value [25]. In fact, at any load step after attaining the critical damage state, the remaining fraction of internal forces applied to nodes of the considered element at crack tip, γ, is given by $\gamma = 1.0 - [(D^*-D_0^*)/\lambda D_0]$, where the D_0^* is the average deformed cell height normal to the crack plane when f is equal to f_c, D^* is the actual deformed cell height and λD_0 represents the allowable elongation of the cell size from the critical condition up to the final cell collapse ($\gamma = 0$), with respect to the undeformed cell height [25]. Beside these parameters it is obviously necessary to know the mechanical properties of the base material (Young modulus, E, Poisson ratio, ν, yielding stress, σ_0, strain hardening, n), or its stress-strain relationship (σ-ε curve).

The investigated material has been the aluminium alloy 2024 T3 (Table I). On the base of this data, the fitting of Tvergaard's parameters was performed by comparing two different numerical models under opportune boundary traction; the obtained values are $q_1 = 1.33$; $q_2 = 0.956$ and $q_3 = 1.77$, confirming the usual assumption $q_3=q_1^2$. In that phase of the fitting process, the nucleation phenomena has not been considered and the f_c value has been used only to determine the last point of comparison between the stress-

strain curves of the two models without any influence on the transferring of the evaluated parameters to the considered fitting process. The second phase of the GT model parameters calibration process consists in the determination of the nucleation (ε_N, S_N, f_N) and macro-mechanical (D_0, f_0, f_c) parameters. Experimental data related to the considered material are needed to reach this aim, regarding both a metallographic analysis [9] and an R-curve of the material under examination [18], [26], [27]. For what concerns the metallographic analysis, the defect distribution in the base material is necessary to choose a first attempt value of the computational cell size, D_0 and of the initial void volume fraction, f_0, to be used in the calibration process. As it is possible to observe from the data recorded in Table II [9], particles or dispersoids are found, which, as it is known, are a cause for void nucleation and therefore can be considered as initial void volume fraction (f_0 = 2.1%). The average distance between the two biggest (> 10 μm) particles is 82.89 μm, which should be approximately the size of the computational cell.

TABLE II
RESULTS FROM METALLOGRAPHIC ANALYSIS

Equivalent diameter [μm]	Volume fraction	Standard deviation	Nearest Neighbour [μm]	Nearest Neighbour (st dv) [μm]
All Sizes	2,10	0,40	8,58	5,37
1:2	0,18	0,06	15,62	10,78
2:3	0,29	0,07	20,95	13,07
3:4	0,33	0,09	28,23	17,69
4:6	0,49	0,14	26,38	14,85
6:8	0,35	0,15	43,01	25,19
8:10	0,22	0,15	69,60	42,43
10+	0,24	0,24	82,89	54,35

Equivalent diameter [μm]	Minimum separation distance [μm]	Minimum separation distance (st dv) [μm]	Av. size of particles in size category
All Sizes	5,78	5,30	2,38
1:2	14,05	11,03	1,46
2:3	18,27	13,33	2,47
3:4	24,54	18,17	3,44
4:6	20,82	15,02	4,85
6:8	35,00	25,76	6,84
8:10	59,25	43,54	8,85
10+	67,90	55,79	12,09

With regard to this proposal it must be said that the smaller the computational cell size, the better is the agreement between the experimental and numerical results, but in order to approach the study of complex full scale structures a too small size of the computational cell may constitute a serious problem for what concerns the computational time; therefore, on the basis of the results reported in [28] and of numerical calculations performed by the authors in order to asses those results, a computational cell size D_0 = 100 μm has been considered. In order to calibrate f_0 and f_c parameters, numerical data have been fitted to the experimental ones represented by the R-curve of a central cracked plate under remote traction [18], whose dimensions are 500 mm x 500 mm, with a thickness of 1.28 mm and an initial crack size of 99.6 mm (Fig. 3); the obtained final values are respectively 0.025 and 0.12. In the same phase of parameters calibration, ε_N, S_N and f_N values have been determined, obtaining ε_N = 0.09, S_N = 0.045 and f_N = 0.11. The advantage in the use of such a kind of specimen instead of a compact test specimen to characterize experimentally the material toughness is to provide an easier full scale components [3], avoiding the difficulties due to the yielding scale at crack tip [29], [30].

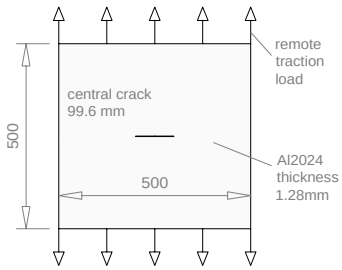

Fig. 3 Fitting parameters panel

V. STIFFENED PANEL: EXPERIMENTAL TEST AND NUMERICAL SIMULATIONS

The values obtained through the calibration process discussed in the previous section have been used to perform calculation of the R-curve of a flat stiffened panel of the Fig. 1. By considering just one crack in the middle bay of initial size a_0 equal to 120 and 150 mm, the results reported in Figs. 4 and 5 have been carried out from both numerical and experimental analyses. As it is possible to observe, numerical results are in very good agreement with the experimental ones.

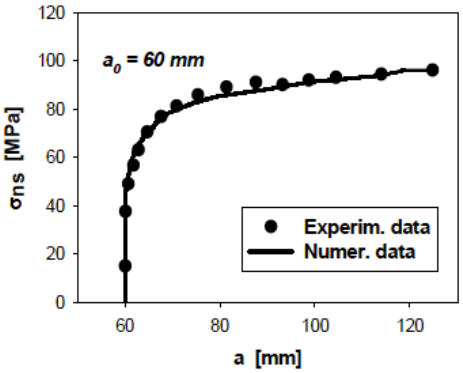

Fig. 4 Stress vs. Half crack length

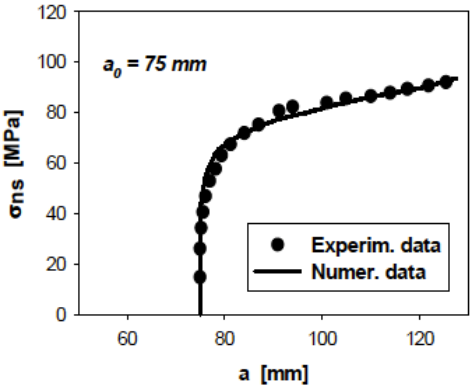

Fig. 5 Stress vs. Half crack length

In the proposed application of the SDI procedure, such full panel has been considered where a central through-crack is assumed to exist, with an initial length of 20 mm. The pitch between the two stringers and their heights has been considered as design variables. As natural variability ± 10.0 mm for the stringers pitch and of ± 0.4 mm for the stringers

height have been assumed, while the engineering intervals of variability have considered to be respectively [306 ÷374 mm] and [1.03 ÷ 3.09 mm]. An increment of the maximum value of the residual strength curve (Rmax) of the 12 % with a success probability greater than 0.80 has been assumed as the target.

VI. Analysis of Results and Conclusion

A total of 6 runs, each one of 15 shots, have been considered adequate to satisfy the target, even if at the end of the procedure an extended MC must be performed in order to assess the obtained results from the 15 shots of the last satisfying run. In the following Figs. 6 and 7 the design variables vs. the maximum value of the residual strength has been illustrated. In correspondence to these two plots we recorded in Fig. 8 the values assumed by the maximum value of the R-curve for each shot. In the same figure the reference value (obtained by considering the initial nominal value of the design variables) of the maximum value of the R-curve is reported together with the target value (dashed line). As it is possible to observe, 9 of the 15 shots of the 5th run overcame the target value; it means that by using the corresponding mean value of the design variable the probability to satisfy the target is of about 0.60. Therefore, another run (the 6th) has been carried out and just one shot doesn't overcome the target value, so that the approximate probability to satisfy the target is about 0.93. The mean value of the design variables in the 6th run is respectively 316.6 mm for the stringer pitch and 2.86 mm for the stinger height; the mean value of the output variable is 122000 N. An extended MC (75 trials) has been performed on the basis of the statistics of the 6th run and the results showed in the Fig. 9 have been obtained, in terms of the maximum values of the residual strength obtained for each trial; in Fig. 10 its mean value and standard deviation vs. the number of the trial have been recorded.

The new mean of the output variable is 121800 N with a standard deviation of 2500 N and the probability to satisfy the target is exactly 0.81. At the end, in the last Fig. 11, the six R-curves corresponding to the six best shots for each run are reported, together with the reference R-curve.

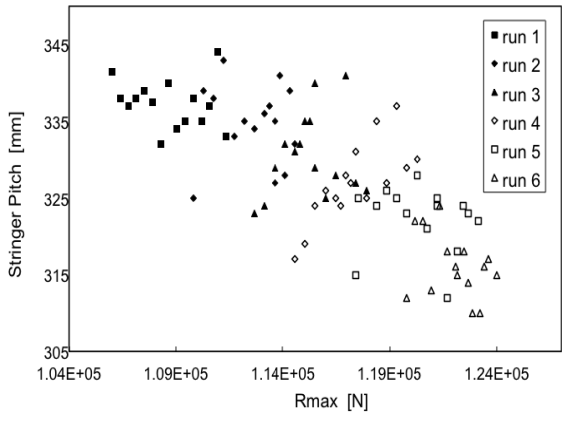

Fig. 6 Design variable vs. output variable

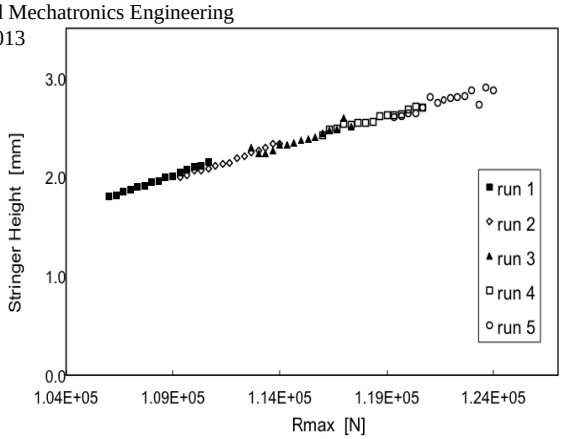

Fig. 7 Design variable vs. output variable

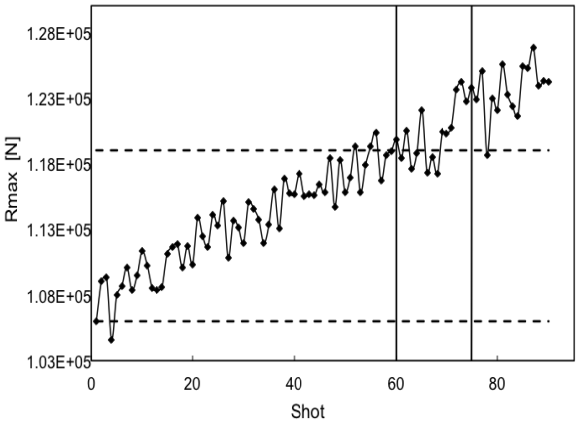

Fig. 8 Output variable vs. shots per run

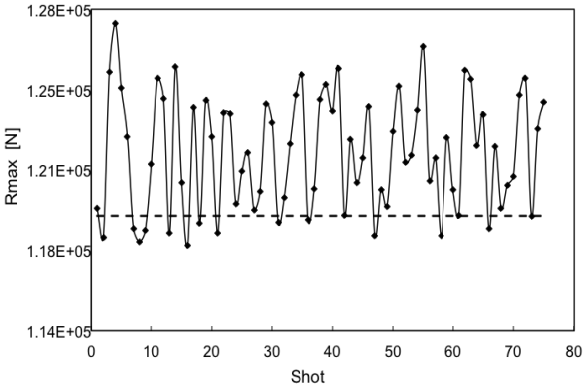

Fig. 9 Output var. vs. shots - extended MC

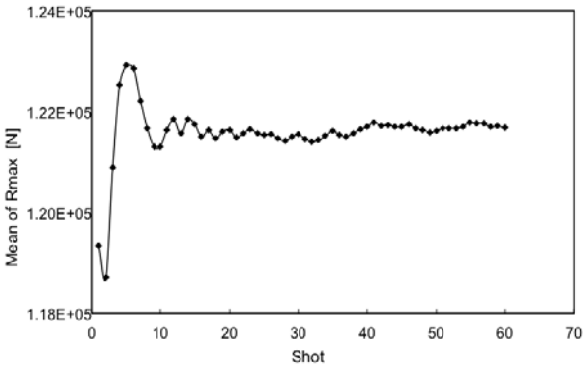

Fig. 10 Mean of output variable vs. shots

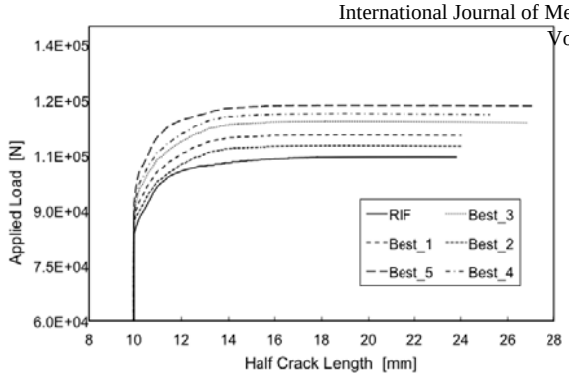

Fig. 11 Mean of output variable vs. shots

VII. Conclusion

The numerical Gurson-Tvergaard micromechanical damage model has been applied to predict the R-curve of a full scale flat stiffened panel made of Al alloy 2024 T3 LT, after calibrating its parameters by means of a phenomenological fitting procedure between numerical and experimental results. The obtained values of those parameters allowed the GT model, in the version implemented in the WARP 3D code, to predict the R-curve of the analysed component very well.

References

[1] R. Mahnken, "Theoretical, numerical and identification aspects of a new model class for ductile damage" in *International Journal of Plasticity*, vol. 18, Ed. Amsterdam, NL: Elsevier, 2002, pp. 801-831.

[2] L. Xia, C. F. Shih, J. W. Hutchinson, "A computational approach to ductile crack growth under large scale yielding conditions" in *Journal of the Mechanics and Physics of Solids*, vol. 43-3, Ed. Amsterdam, NL: Elsevier, 1995, pp. 389-413.

[3] O. Chabanet, D. Steglich, J. Besson, V. Heitmann, D. Hellmann, W. Brocks, "Predicting crack growth resistance of aluminium sheets" in *Computational Materials Science*, vol. 26, Ed. Amsterdam, NL: Elsevier, 2003, pp. 1-12.

[4] O. Kintzel, S. Khan, J. Mosler "A novel isotropic quasi-brittle damage model applied to LCF analyses of Al2024" in *International Journal of Fatigue*, vol. 32-12, Ed. Amsterdam, NL: Elsevier, 2010, pp. 1948-1959.

[5] J. Faleskog, X. Gao, C. F. Shih, "Cell model for nonlinear fracture analysis – I Micromechanics calibration" in *International Journal of Fracture*, vol. 89, Ed. Heidelberg, D: Springer, 1998, pp. 355-373.

[6] F. Scheyvaerts, P.R. Onck, C. Teko□lu, T. Pardoen, "The growth and coalescence of ellipsoidal voids in plane strain under combined shear and tension" in *Journal of the Mechanics and Physics of Solids,* vol. 59-2, Ed. Amsterdam, NL: Elsevier, 2010, pp. 373-397.

[7] L. Gurson, "Continuum theory of ductile rupture by void nucleation and growth: part I - yield criteria and flow rules for porous ductile media" in *Journal of Engineering Materials and Technology – T. ASME*, vol. 99-1, Ed. New York, USA, 1977, pp. 2-15.

[8] V. Tvergaard, "Influence of void nucleation on ductile shear fracture at a free surface" in *Journal of the Mechanics and Physics of Solids*, vol. 30, Ed. Amsterdam, NL: Elsevier, 1982, pp. 399-425.

[9] J.S Robinson, Presentation on the IDA meeting in Geesthacht 22-23 June 2005, University of Limerick (2005).

[10] F. Caputo, G. Lamanna, A. Soprano, "Stochastic improvement of the residual strength of a stiffened panel" in *Key Engineering Materials*, vol. 348-349, Ed. Durnten-Zurich, CH: Trans Tech Publications Inc., 2007, pp. 301-304.

[11] C. Zang, M.I. Friswell, J. E. Mottershead, "A review of robust optimal design and its application in dynamics" in *Computers and Structures*, vol. 83, Ed. Amsterdam, NL: Elsevier, 2005, pp. 315-326.

[12] T. E. Murphy, K. L. Tsui, J. K. Allen, "A review of robust design methods for multiple responses" in *Research in Engineering Design*, vol. 16, Ed. Heidelberg, D: Springer, 2005, pp. 118-127.

[13] F. Caputo, A. Soprano, G. Monacelli, "Stochastic design improvment of an impact absorber" in *Latin American J. of Solids and Structures*, vol. 3, Ed. Sao Paulo, BR: Lajss, 2006, pp. 41-53.

[14] A. Soprano, F. Caputo, "Building a risk assessment procedure" in *Structural Durability & Health Monitoring*, vol. 2, n. 1, Ed. Duluth GA, USA: Tech Science Press, 2006, pp. 51-68.

[15] R. Citarella, A. Apicella, "Advanced design concepts and maintenance by integrated risk evaluation for aerostructures" in *Structural Durability & Health Monitoring*, vol. 2, n. 3, Ed. Duluth GA, USA: Tech Science Press, 2006, pp. 183-196.

[16] I. Doltsinis, F. Rau, M. Werner, "Analysis of random systems", Ed. I. Doltsinis, Barcelona, E: CIMNE 2004, pp. 9-149.

[17] E. Armentani, R. Citarella, R. Sepe, "FML Full scale aeronautic Panel under multiaxial fatigue: experimental test and DBEM simulation" in *Engineering Fracture Mechanics*, vol. 78, Ed. Amsterdam, NL: Elsevier, 2011, pp. 1717-1728.

[18] H. J. ten Hoeve, L. Schra, A. L. P. J. Michielsen, H. Vlieger, "Residual strength test on stiffened panels with multiple-site damage", report n: DOT/FAA/AR-98/53, U.S. Department of Transportation, USA, 1999.

[19] G. Lamanna, F. Caputo, A. Soprano, "Geometrical parameters influencing a hybrid mechanical coupling", in *Key Engineering Materials*, vol. 525-526, Ed. Durnten-Zurich, CH: Trans Tech Publications Inc., 2012, pp. 161-164.

[20] A. Soprano, F. Caputo, A. Grimaldi, "A numerical Investigation about the effects of the riveting operation on the strength of joints" in *Key Engineering Materials*, vol. 348-349, Ed. Durnten-Zurich, CH: Trans Tech Publications Inc., 2007, pp. 265-268.

[21] G. Lamanna, F. Caputo, A. Soprano, "Handling of composite-metal interface in a hybrid mechanical coupling", in *AIP American Institute of Physics conference proceedings*, vol. 1459, Ed. Melville New York, USA: American Institute of Physics, 2012, pp 353-356.

[22] G. Lamanna, F. Caputo, A. Soprano, "Effects of tolerances on the structural behaviour of a bolted hybrid joint", in *Key Engineering Materials*, vol. 488-489, Ed. Durnten-Zurich, CH: Trans Tech Publications Inc., 2012, pp. 565-568.

[23] G. Lamanna, F. Caputo, A. Soprano, "Numerical modelling and simulation of a bolted hybrid joint", in *Structural Durability & Health Monitoring*, vol. 7, n. 4, Ed. Duluth GA, USA: Tech Science Press, 2011, pp. 283-296.

[24] G. Lamanna, F. Caputo, F.M. Pannullo, G. De Angelis, "A methodological approach to the tolerance problems during the assembly process of deformable bodies", in *Key Engineering Materials*, vol. 488-489, Ed. Durnten-Zurich, CH: Trans Tech Publications Inc., 2012, pp. 557-560.

[25] A. S. Gullerud, K. C. Koppenhoefer, A. Roy, R. H. Dodds, jr., B. Healy, S. RoyChowdhury, M. Walters, B. Bichon, K. Cochran, A. Carlyle, J. Sobotka, M. Messner, Warp3D Release 17.3.2 3D Dynamic Nonlinear Fracture analysis of Solids Using Parallel Computers, User and theoretical manual, (University of Illinois), 2012.

[26] F. Caputo, G. Lamanna, A. Soprano, "Numerical investigation on the crack propagation in a flat stiffened panel" in *Key Engineering Materials*, vol. 324-325, Ed. Durnten-Zurich, CH: Trans Tech Publications Inc., 2006, pp. 1039-1042.

[27] C. Calì, R. Citarella, "Residual strength assessment for a butt-joint in MSD condition" in *Advences in Egineering Software*, vol. 35, Ed. Amsterdam, NL: Elsevier, 2004, pp. 373-382.

[28] D. Steglich, T. Siegmund, W. Brocks, "Micromechanical modeling of damage due to particle cracking in reinforced metals" in Computational Materials Science, vol. 16, Ed. Amsterdam, NL: Elsevier, 1999, pp. 404-413.

[29] F. Caputo, G. Lamanna, A. Soprano, "The plastic zone size at short cracks tip" in *Engineering Fracture Mechanics*, Ed. Amsterdam, NL: Elsevier, 2012, doi: 10.1016/j.engfracmech.2012.09.030.

[30] F. Caputo, G. Lamanna, A. Soprano, "An analytical formulation for the plastic deformation at the tip of short cracks" in *Procedia Engineering*, vol. 10, Ed. Amsterdam, NL: Elsevier, 2011, pp. 2988-2993.